
FIRING RATE OF THE LEAKY INTEGRATE-AND-FIRE NEURON WITH STOCHASTIC CONDUCTANCE-BASED SYNAPTIC INPUTS WITH SHORT DECAY TIMES

A PREPRINT

Timothy D. Oleskiw
Center for Neural Science
New York University
New York City, NY, USA

Wyeth Bair*
Department of Biological Structure
University of Washington
Seattle, WA, USA

Eric Shea-Brown*
Department of Applied Mathematics
University of Washington
Seattle, WA, USA

Nicolas Brunel
Departments of Neurobiology and Physics
Duke University
Durham, NC, USA

February 27, 2020

ABSTRACT

We compute the firing rate of a leaky integrate-and-fire (LIF) neuron with stochastic conductance-based inputs in the limit when synaptic decay times are much shorter than the membrane time constant. A comparison of our analytical results to numeric simulations is presented for a range of biophysically-realistic parameters.

Introduction

Information processing within neural networks is widely considered to be achieved by circuit computations in which the firing rate, either of a single neuron or populations of functionally similar neurons, serves as the fundamental variable [3]. Therefore, by understanding how basic mathematical operations like addition and multiplication are applied to firing rates in networks, we may gain insight into fundamental mechanisms of neural computation [1, 7, 15, 18].

Multiple studies have demonstrated that a neuron's output rate can be significantly affected by the *timescale* of fluctuating input, which can be modulated by factors such as the spike timing and correlation of upstream activity [13] or by the kinetics of synaptic filtering [14]. Input timescale has been shown in several studies to impact the firing rates of model neurons [5, 6, 8, 12, 13] as well as the gain and phase of their frequency response [4, 8].

Most of our present insights about how the time scales of synaptic inputs affect output firing rate come from analytic solutions for the firing rate of leaky integrate-and-fire (LIF) neurons under stochastic input, in both the short

[6, 8] and long input time limits [13]. Recently, the firing rate of a LIF neuron for arbitrary input time scale was obtained as a solution of a Fredholm integral equation of the second kind, which can then be solved numerically [17]. However, these studies all use *current based* LIFs, *i.e.*, synaptic input to be injected current. Such a formulation has the advantage of simplicity and may be valid in some physiological limits, but neglects the general dependence of synaptic inputs on membrane potential. These dependencies can be described by the so-called 'conductance-based' formalism wherein synaptic inputs are a product of synaptic conductance times the 'driving force', *i.e.* the difference between membrane potential and the synaptic reversal potential.

Here, we present a generalization of the calculations described in [6, 8] to a LIF model with conductance-based synaptic inputs, when the input correlation time constant is much shorter than the membrane time constant.

Model formulation

A ubiquitous model of a one-compartmental neuron with conductance-based synaptic inputs is defined by its membrane potential $V(t)$, and excitatory (E) and inhibitory (I)

*These authors contributed equally to this work.

total conductances $g_e(t)$ and $g_i(t)$, whose dynamics obey

$$C \frac{d}{dt} V = g_l(v_l - V) + g_e(v_e - V) + g_i(v_i - V) \quad (1)$$

$$\tau_e \frac{d}{dt} g_e = -g_e + \mu_e + \sigma_e \sqrt{\tau_e} \eta_e(t) \quad (2)$$

$$\tau_i \frac{d}{dt} g_i = -g_i + \mu_i + \sigma_i \sqrt{\tau_i} \eta_i(t), \quad (3)$$

where C is the membrane capacitance, g_l the leak conductance, v_l the resting membrane potential, v_e and v_i are synaptic reversal potentials, τ_e and τ_i are synaptic decay time constants, μ_e and μ_i are mean synaptic conductances, σ_e and σ_i are the amplitude of the fluctuations, and η_e and η_i Gaussian white noise, each for the E and I conductances, respectively [2, 11]. These equations are complemented with the usual threshold-and-reset mechanism, *i.e.* a spike is emitted whenever the voltage reaches a threshold v_t and the voltage is then reset instantaneously to v_r . Equations (2) and (3) are obtained from Poisson synaptic inputs using a diffusion approximation, *i.e.* a shot noise process approximated by a continuous Gaussian process with the same mean and variance. As the post-synaptic potentials evoked by neural inputs are not instantaneous, timescales τ_e and τ_i are chosen to mimic excitatory and inhibitory neurotransmitter kinetics.

Equations (2)-(3) are difficult to analyze mathematically because the computation of quantities of interest (mean firing rate, distribution of membrane potential) involves solving a 3D Fokker-Planck equation with complicated boundary conditions at threshold and reset. A first simplification consists in considering that only a single type of conductance fluctuates (here, E), while the other is constant in time, $g_i = \mu_i$, leading to the two-variable system

$$C \frac{d}{dt} V = g_l(v_l - V) + g_e(v_e - V) + \mu_i(v_i - V) \quad (4)$$

$$\tau_e \frac{d}{dt} g_e = -g_e + \mu_e + \sigma_e \sqrt{\tau_e} \eta(t).$$

Rewriting $g_e = \mu_e + \sigma_e z$, and $\tau_e = \tau_s$, we obtain

$$\tau_m \frac{d}{dt} V = A(V) + \frac{1}{k} B(V) z \quad (5)$$

$$\tau_s \frac{d}{dt} z = -z + \sqrt{\tau_s} \eta(t),$$

where the membrane time constant $\tau_m = C/g_l$, $k = \sqrt{\tau_s/\tau_m}$, and

$$A(V) = v_l - V + \frac{\mu_e}{g_l}(v_e - V) + \frac{\mu_i}{g_l}(v_i - V) \quad (6)$$

$$B(V) = \frac{\tilde{\sigma}_e}{g_l}(v_e - V),$$

where $\tilde{\sigma}_e = k\sigma_e$. Note that $\tilde{\sigma}_e$ should be of order 1 in the limit $k \rightarrow 0$ for conductance fluctuations to lead to fluctuations of the voltage of finite variance. This means that σ_e should be of order $1/k$ in that limit. We now seek to approximate the firing rate r of system (5) by solving for the mean number of threshold crossings (spikes) per unit time (seconds) under general input conditions.

Simulation methods

Simulations of all spiking LIF models were performed in MATLAB R2013b. Dynamics were evaluated numerically with the forward Euler method at a time step of 10 microseconds. After crossing threshold, a spike was recorded and membrane voltage was forced to reset instantaneously. Spike-rate response was determined from the mean spike frequency over a 100 second stimulation duration. Code is available upon request.

Results

We now demonstrate the key steps to approximating the firing rate of the general LIF system described by (5). The associated equilibrium Fokker-Planck equation for the distribution $P(V, z)$ of voltage V and input z is given by [9]

$$\mathcal{L}P - kz \frac{\partial}{\partial V}(B(V)P) - k^2 \frac{\partial}{\partial V}(A(V)P) = 0, \quad (7)$$

with the differential operator \mathcal{L} defined as

$$\mathcal{L}P = \frac{1}{2} \frac{\partial^2 P}{\partial z^2} + \frac{\partial}{\partial z}(zP). \quad (8)$$

The probability flux in voltage V is therefore

$$J_V = \frac{1}{\tau_m} \left(A(V) + B(V) \frac{z}{k} \right) P, \quad (9)$$

which cannot be negative at spiking threshold $V = V_{th}$, giving rise to the boundary conditions

$$P(V_{th}, z) = 0 \quad z < -k \frac{A(V_{th})}{B(V_{th})} \quad (10)$$

$$P(V_{th}, z) \geq 0 \quad z > -k \frac{A(V_{th})}{B(V_{th})}.$$

The strategy is to find solutions in boundary layers, as in [10] and [8]. We compute the solution in three regions: (i) in the *outer* region far from both threshold and reset, (ii) in the *threshold layer* when V is close to emitting a spike, and (iii) in the *reset layer* when V is close to the reset potential.

Outer solution

The outer solution, far from reset and threshold, is obtained by expanding the probability distribution P in powers of k , *i.e.* $P = P_0 + kP_1 + k^2P_2 + \dots$. Substituting this expansion into (7), we find a recurrence relation for the distribution terms P_i given by

$$\mathcal{L}P_0 = 0$$

$$\mathcal{L}P_1 = z \frac{\partial}{\partial V}(BP_0)$$

$$\mathcal{L}P_2 = z \frac{\partial}{\partial V}(BP_1) + \frac{\partial}{\partial V}(AP_0)$$

$$\dots,$$
(11)

which leads to

$$\begin{aligned}
P_0 &= \frac{e^{-z^2}}{\sqrt{\pi}} Q_0(V) \\
P_1 &= \frac{e^{-z^2}}{\sqrt{\pi}} Q_1(V) - \frac{ze^{-z^2}}{\sqrt{\pi}} \frac{\partial}{\partial V} (BQ_0) \\
P_2 &= \frac{e^{-z^2}}{\sqrt{\pi}} Q_2(V) - \frac{ze^{-z^2}}{\sqrt{\pi}} \frac{\partial}{\partial V} (BQ_1) \\
&\quad + \frac{z^2 e^{-z^2}}{2\sqrt{\pi}} \frac{\partial}{\partial V} \left(B \frac{\partial}{\partial V} (BQ_0) \right).
\end{aligned} \tag{12}$$

To find a solution for P_2 that satisfies the boundary conditions on z (i.e., both P_2 and $\partial P_2 / \partial z$ should go to zero in both $z \rightarrow \pm\infty$ limits) we need to impose the solvability condition

$$\frac{1}{2} \frac{\partial}{\partial V} \left(B(V) \frac{\partial (B(V)Q_0)}{\partial V} \right) - \frac{\partial (A(V)Q_0)}{\partial V} = 0, \tag{13}$$

which is solved for Q_0 . As expected, (13) coincides with the Fokker-Plank equation in the white noise limit using Stratonovich calculus. Going to third order, we find that Q_1 obeys (13) as well. Thus,

$$\begin{aligned}
Q_0(V) &= \begin{cases} \alpha_0 R(V) & V < V_{re} \\ \beta_0 R(V) + \gamma_0 S(V) & V > V_{re} \end{cases} \\
Q_1(V) &= \begin{cases} \alpha_1 R(V) & V < V_{re} \\ \beta_1 R(V) + \gamma_1 S(V) & V > V_{re} \end{cases}
\end{aligned} \tag{14}$$

for the voltage reset potential V_{re} , where

$$R(V) = \frac{W(V)}{B(V)} \tag{15}$$

and

$$S(V) = \frac{W(V)}{B(V)} \int_V^{V^t} \frac{du}{B(u)W(u)} \tag{16}$$

for W given in (31). Furthermore, the solutions Q_0 and Q_1 have to obey the normalization conditions

$$\begin{aligned}
\int Q_0(V) dV &= 1 \\
\int Q_1(V) dV &= 0.
\end{aligned} \tag{17}$$

Inner solutions

Solutions to the inner threshold and reset layers are found using similar techniques. To construct solutions within the threshold layer, we need to transform voltage as $V = V_{th} - kxV_{th}$. It will also be convenient to define a substitution

$$z' = z + k \frac{A(V_{th})}{B(V_{th})}, \tag{18}$$

simplifying the boundary conditions and operator \mathcal{L}' . Therefore, rewriting (7) for the threshold distribution P^T ,

i.e. the probability of the system near spiking threshold V_{th} , we have

$$\begin{aligned}
\mathcal{L}' P^T + z' \frac{\partial P^T}{\partial x} \\
- k \left(\frac{A(V_{th})}{B(V_{th})} \frac{\partial P^T}{\partial z'} + \frac{B(V_{th})}{B(V_{th})} z' \frac{\partial}{\partial x} (x P^T) \right) \\
+ O(k^2) = 0,
\end{aligned} \tag{19}$$

which again can be solved by expanding $P^T = P_0^T + kP_1^T + \dots$, satisfying the boundary condition $P^T(0, z') = 0$ for $z' < 0$. The probability flux at $(0, z')$ is given by $z' P^T(0, z') B(V_{th}) / (\tau_m k)$, implying $P_0^T = 0$. The firing rate terms at zero and first orders are therefore

$$\begin{aligned}
\nu_0 &= \frac{B(V_{th})}{\tau_m} \int_0^\infty z' P_1^T(0, z') dz' \\
\nu_1 &= \frac{B(V_{th})}{\tau_m} \int_0^\infty z' P_2^T(0, z') dz'.
\end{aligned} \tag{20}$$

A solution to P_1^T has previously been found by [10] to be

$$P_1^T = \frac{e^{-z'^2}}{\sqrt{\pi}} \rho_1^T (\tilde{\alpha} + x + z + U(x, z)), \tag{21}$$

where $\tilde{\alpha}$ and $U(x, z)$ are described in [10]. Using the fact that U decays exponentially to zero for large x , and that $\int z e^{-z'^2} U(x, z) = 0$, we conclude that $\rho_1^T = 2\nu_0 \tau_m / B(V_{th})$ [10].

The reset layer can be dealt with exactly in the same way as the threshold layer. One finds the solutions to the left and right of the reset, i.e. V_{re}^- and V_{re}^+ , coincide at zero order, but that the difference between these solutions obeys (21) [4, 8].

Matching outer and inner layers

To match the outer and threshold layers we use the change of variables $V = V_{th} - kxB(V_{th})$, $z' = z + kA(V_{th})/B(V_{th})$. Therefore, the outer solution becomes

$$\begin{aligned}
P(x, z') &= \frac{e^{-z'^2}}{\sqrt{\pi}} \left(Q_0(V_{th}) + k \left[Q_1(V_{th}) \right. \right. \\
&\quad \left. \left. - xB(V_{th})Q_0'(V_{th}) + \frac{z'\gamma_0}{B(V_{th})} \right] \right).
\end{aligned} \tag{22}$$

This solution must match P_1^T in the large x limit. Hence, we have $Q_0(V_{th}) = 0$ which implies $\beta_0 = 0$. We also have

$$\begin{aligned}
\gamma_0 &= 2\nu_0 \tau_m \\
Q_1(V_{th}) &= \tilde{\alpha} \rho_1^T = \frac{2\tilde{\alpha} \nu_0 \tau_m}{B(V_{th})},
\end{aligned} \tag{23}$$

which leads to

$$\beta_1 = \frac{2\tilde{\alpha} \nu_0 \tau_m}{W(V_{th})}. \tag{24}$$

Matching of the reset and outer layers is done in a similar way. One finds that Q_0 has to be continuous in V_{re} , implying

$$\alpha_0 = \int_{V_{re}}^{V_{th}} \frac{du}{B(u)W(u)}, \quad (25)$$

which, together with the normalization condition for Q_0 , leads to the equation for the zeroth order firing rate ν_0 as expected. One then finds that Q_1 is instead discontinuous in V_{re} , with

$$\begin{aligned} Q_1(V_{re}^+) - Q_1(V_{re}^-) &= \tilde{\rho}_1^T \\ &= \beta_1 R(V_{re}) + \gamma_1 S(V_{re}) - \alpha_1 R(V_{re}). \end{aligned} \quad (26)$$

Including now the normalization condition for Q_1 , this gives us two equations for the last two remaining unknowns, γ_1 and α_1 . In particular, we find that

$$\gamma_1 = 4\tilde{\alpha}(\nu_0\tau_m)^2 B(V_{th}) \left(\frac{B(V_{re})^2}{B(V_{th})^2} \psi(V_{re}) - \psi(V_{th}) \right), \quad (27)$$

where

$$\psi(V) = \frac{1}{B(V)W(V)} \int_{-\infty}^V R(u)du. \quad (28)$$

First order correction to the firing rate

The last step is to compute ν_1 . From (20) it would seem that we need to compute P_2^T . Fortunately we only need the term proportional to z in this equation, as it is the only term that contributes to the firing rate. Further, the condition matching the outer and inner solutions requires this term to be proportional to γ_1 . Therefore, the correction is

$$\begin{aligned} \nu_1 &= \frac{\gamma_1}{2\tau_m} \\ &= 2\tilde{\alpha}\nu_0^2\tau_m B(V_{th}) \left(\frac{B(V_{re})^2}{B(V_{th})^2} \psi(V_{re}) - \psi(V_{th}) \right). \end{aligned} \quad (29)$$

As in [6] and [8] we can express the firing rate r as

$$\frac{1}{r} = 2\tau_m \int_{v_{re}^{eff}}^{v_{th}^{eff}} \frac{dz}{B(z)W(z)} \int_{-\infty}^z \frac{W(x)}{B(x)} dx, \quad (30)$$

where

$$W(v) = \exp\left(2 \int^v \frac{A(u)}{B^2(u)} du\right) \quad (31)$$

and where

$$\begin{aligned} v_{th}^{eff} &= v_{th} + B(v_{th}) \frac{\alpha}{2} k \\ v_{re}^{eff} &= v_{re} + \frac{B^2(v_{re})}{B(v_{th})} \frac{\alpha}{2} k \end{aligned} \quad (32)$$

are the effective membrane threshold and reset potentials. Note that $\alpha = -\sqrt{2}\zeta(\frac{1}{2})$ where ζ is the Riemann zeta function [10]. Here, (30) gives the correct two first orders (0th and 1st) in the small k expansion of the firing rate, but also leads to a better approximation of the firing rate in a larger range of values of k : it is guaranteed to stay positive at all values of k , while $r = \nu_0 + k\nu_1$ becomes negative for large k .

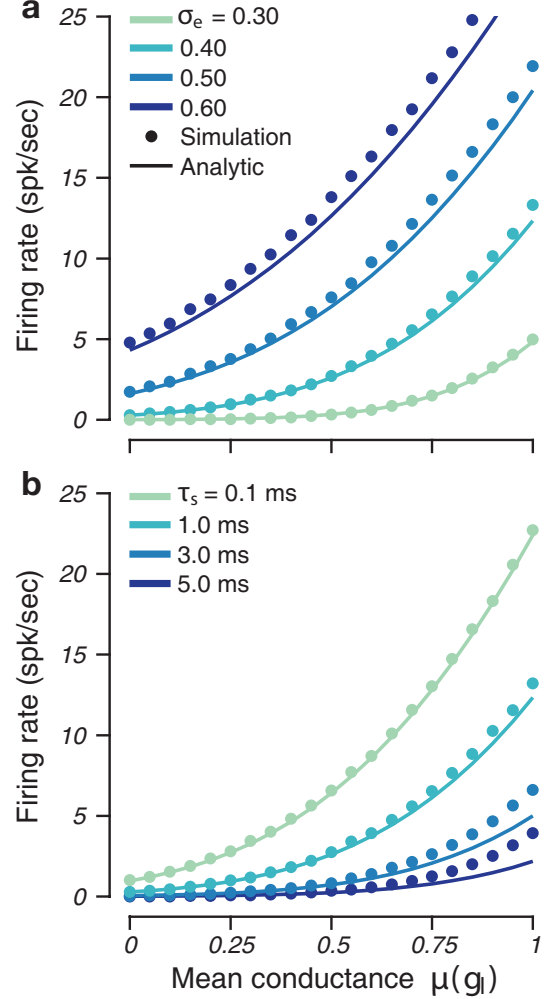


Figure 1: Comparison of the analytic approximation to the firing rate of a neuron described by (5), (6), and (30) to values estimated through numerical simulation. (a) Standard deviation of excitatory conductance σ_e is varied for fixed timescale $\tau_s = 1$ ms, and (b) synaptic timescale is varied for fixed $\sigma_e = 0.40 g_l$.

Comparison of approximation to numeric simulation

In Fig. 1 we demonstrate the accuracy of our approximation by simulating a conductance-based LIF neuron described by (6) using the following biophysically-realistic parameters: the membrane time constant τ_m is $\tau_m = C/g_l = 37$ ms, the leak conductance is $g_l = 20$ nS, with reversal potentials $v_l = -70$ mV, $v_e = 0$ mV, and $v_i = -80$ mV. Membrane threshold and reset potentials are $v_{th} = -52$ mV and $v_{re} = v_l$, respectively [2].

A tonic inhibitory conductance of $3g_l$ is included to prevent spiking under noisy excitatory input of zero mean conductance. Further, we mimic a small amount of balanced synaptic input [2] by including additional excitatory and inhibitory conductance, leading us to take $\mu_i = 3.3g_l$ and $\mu_e = (0.1 + \mu)g_l$. Our qualitative results, however, are

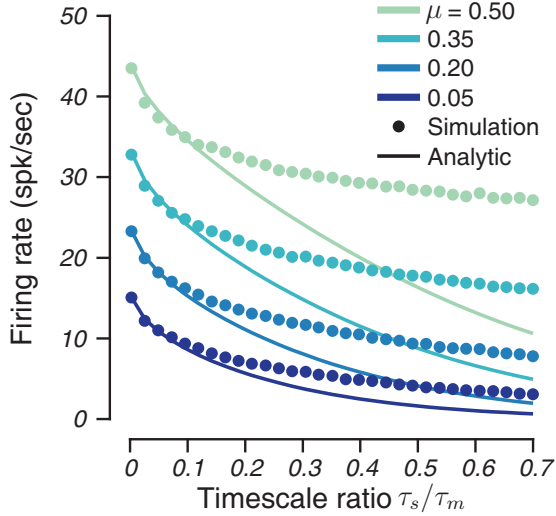


Figure 2: Comparison of simulation results with the analytic approximation (30) for (5) and (6) in the case of small balanced synaptic input, *i.e.* $\mu_i = 0.3g_l$ and $\mu_e = (0.1 + \mu)g_l$ for $\sigma_e = 0.40$. Note that firing rates exhibit a $\sqrt{\tau_s}^{-1}$ relationship for $\tau_s \ll 1$ across multiple levels of mean excitation μ .

insensitive to this parameterization. Fig. 1 shows general agreement over a range of parameter values, although the approximation begins to break down as τ_s increases, consistent with the fact that our analytic formula is valid to first order in $k = \frac{\tau_s}{\tau_m}$. However, the approximation holds for a realistic membrane constant and input timescales $\tau_s \lesssim 5$ ms, similar to estimated decay constants for glutamate and AMPA receptors. [16].

The effect of synaptic timescale on the firing rate is examined further in Fig. 2. Here, multiple levels of mean input μ drive the neuron into a sub- and supra-threshold regime while synaptic fluctuation $\sigma_e = 0.4g_l$ is fixed. We note that for small k , *i.e.* $\frac{\tau_s}{\tau_m} \lesssim 0.1$, the approximation closely matches simulation and captures the fact that firing rates are proportional to $\sqrt{\tau_s}^{-1}$.

Discussion

In this study we have built upon a previously known approximation to the firing rate of LIF neurons to cover the case of conductance-based input. Importantly, we find the method to give a good approximation of the firing rate under many biophysically-realistic inputs, providing an analytic tool for studying the response of such neurons. While we leave a quantitative analysis of approximation error as a topic of future study, the strong qualitative agreement to simulation suggests our derivation to be useful over a range of parameters. In particular, this work provides an analytic tool for investigating how the statistical properties of input affect a neuron's firing rate, and thus for understanding a neuron's computational properties.

References

- [1] A. Angelucci and P. C. Bressloff. Chapter 5 Contribution of feedforward, lateral and feedback connections to the classical receptive field center and extra-classical receptive field surround of primate V1 neurons. *Progress in Brain Research*, 154(SUPPL. A):93–120, 2006.
- [2] A. Ayaz and F. S. Chance. Gain modulation of neuronal responses by subtractive and divisive mechanisms of inhibition. *J Neurophysiol*, 101(2):958–68, feb 2009.
- [3] H. B. Barlow. Single units and sensation: A neuron doctrine for perceptual psychology? *Perception*, 1(4):371–394, 1972.
- [4] N. Brunel, F. S. Chance, N. Fourcaud, and L. F. Abbott. Effects of synaptic noise and filtering on the frequency response of spiking neurons. *Physical Review Letters*, 86:2186–2189, 2001.
- [5] N. Brunel and P. E. Latham. Firing rate of the noisy quadratic integrate-and-fire neuron. *Neural computation*, 15(10):2281–306, oct 2003.
- [6] N. Brunel and S. Sergi. Firing frequency of leaky integrate-and-fire neurons with synaptic current dynamics. *Journal of theoretical biology*, 195:87–95, 1998.
- [7] M. Carandini and D. J. Heeger. Normalization as a canonical neural computation. *Nature reviews. Neuroscience*, 13(1):51–62, nov 2011.
- [8] N. Fourcaud and N. Brunel. Dynamics of the firing probability of noisy integrate-and-fire neurons. *Neural computation*, 14:2057–2110, 2002.
- [9] C. Gardiner. *Stochastic Methods: A Handbook for the Natural and Social Sciences*. Springer Berlin Heidelberg, 2009.
- [10] P. S. Hagan, D. A. Doering, and C. D. Levermore. Mean Exit Times for Particles Driven by Weakly Colored Noise. *SIAM J. Appl. Math.*, 49(5):1480–1513, 1989.
- [11] C. Ly and B. Doiron. Divisive gain modulation with dynamic stimuli in integrate-and-fire neurons. *PLoS computational biology*, 5(4):e1000365, apr 2009.
- [12] S. J. Mitchell and R. A. Silver. Shunting inhibition modulates neuronal gain during synaptic excitation. *Neuron*, 38(3):433–45, may 2003.
- [13] R. Moreno, J. de la Rocha, A. Renart, and N. Parga. Response of Spiking Neurons to Correlated Inputs. *Physical Review Letters*, 89(28):288101, dec 2002.
- [14] C. O'Donnell and M. C. W. van Rossum. Systematic analysis of the contributions of stochastic voltage gated channels to neuronal noise. *Frontiers in computational neuroscience*, 8(September):105, jan 2014.
- [15] T. K. Sato, M. Häusser, and M. Carandini. Distal connectivity causes summation and division across mouse visual cortex. *Nature neuroscience*, 17(1):30–2, 2014.
- [16] N. Spruston, P. Jonas, and B. Sakmann. Dendritic glutamate receptor channels in rat hippocampal CA3 and CA1 pyramidal neurons. *The Journal of Physiology*, 482(2):325–352, jan 1995.
- [17] C. Van Vreeswijk and F. Farkhooi. Fredholm theory for the mean first-passage time of integrate-and-fire oscillators with colored noise input. *Physical Review E*, 100(6):60402, 2019.
- [18] A. J. Yu, M. A. Giese, and T. A. Poggio. Biophysically plausible implementations of the maximum operation. *Neural computation*, 14(12):2857–81, dec 2002.